

Article

# Geochemical Characteristics of Shallow Groundwater in Jiaoshiba Shale Gas Production Area: Implications for Environmental Concerns

Yiman Li <sup>1</sup>, Tianming Huang <sup>1,\*</sup>, Zhonghe Pang <sup>1,\*</sup>, Yingchun Wang <sup>1,2</sup> and Chao Jin <sup>3</sup>

<sup>1</sup> Key Laboratory of Shale Gas and Geoenvironment, Institute of Geology and Geophysics, Chinese Academy of Sciences, Beijing 100029, China; liyiman@mail.iggcas.ac.cn (Y.L.); wyc185@163.com (Y.W.)

<sup>2</sup> University of Chinese Academy of Sciences, Beijing 100049, China

<sup>3</sup> Hebei University of Engineering Handan, Handan 056038, Hebei, China; baobei181920@126.com

\* Correspondence: tmhuang@mail.iggcas.ac.cn (T.H.); z.pang@mail.iggcas.ac.cn (Z.P.); Tel.: +86-10-8299-8276 (T.H.); +86-10-8299-8613 (Z.P.)

Academic Editor: Wilhelm Puttmann

Received: 8 September 2016; Accepted: 16 November 2016; Published: 28 November 2016

**Abstract:** The geochemical characteristics of shallow groundwater are essential for environmental impact studies in the shale gas production area. Jiaoshiba in the Sichuan basin is the first commercial-scale shale gas production area in China. This paper studied the geochemical and isotopic characteristics of the shallow groundwater of the area for future environmental concerns. Results show that the average pH of the shallow groundwater is 7.5 and the total dissolved solids (TDS) vary from 150 mg/L to 350 mg/L. The main water types are HCO<sub>3</sub>-Ca and HCO<sub>3</sub>-Ca·Mg due to the carbonates dissolution equilibrium in karst aquifers. The concentrations of major ions and typical toxic elements including Mn, Cr, Cu, Zn, Ba, and Pb are below the drinking water standard of China and are safe for use as drinking water. The high nitrate content is inferred to be caused by agricultural pollution. The shallow groundwater is recharged by local precipitation and flows in the vertical circulation zone. Evidences from low TDS, water isotopes, and high <sup>3</sup>H and <sup>14</sup>C indicate that the circulation rate of shallow groundwater is rapid, and the lateral groundwater has strong renewability. Once groundwater pollution from deep shale gas production occurs, it will be recovered soon by enough precipitation.

**Keywords:** Jiaoshiba; hydrogeochemical characteristics; shale gas production; potential contamination; Sichuan basin

## 1. Introduction

Shale gas existing in low-permeability reservoirs has rapidly emerged as one of the vital sources of unconventional energies, and the development of multi-horizontal drilling and hydraulic fracturing technologies has paved the way for economic exploitation of shale gas resources [1,2]. Environmental concerns from shale gas production have drawn more and more attention from the public and regulatory bodies, in particular the composition and fate of the fluid generated by hydraulic fracturing processes in deep reservoirs [3–5]. Studies of typical shale gas production projects such as Marcellus and Fayetteville, both in the USA, show that contamination of groundwater system does probably exist. A relationship between methane concentrations in shallow groundwater and the proximity of drinking water wells to shale gas drilling sites in northeastern Pennsylvania is demonstrated in the Marcellus shale basin, indicating the contamination of shallow groundwater by stray gas [6]. The total dissolved solids (TDS) of flowback fluid after hydraulic fracturing always increase dramatically with time and can reach up to 300 g/L [7–11].

Shale gas exploration in China began in 2005 and has established three demonstration areas of marine facies shale production in the Sichuan basin since 2010 [12,13]. More than 800 boreholes have been drilled and 270 of those were fractured to produce shale gas. The shale gas resource geological reserve in the Wufeng-Longmaxi formation of the Silurian period discovered in the Fuling, Changyuan, and Weiyuan areas of the Sichuan basin was evaluated to be  $5441 \times 10^8 \text{ m}^3$  and its annual production yield is higher than  $40 \times 10^8 \text{ m}^3$  [14–17]. Shale gas production is already occurring and is at early stages compared with production abroad. Thus, geochemical baseline establishment and long-term monitoring in the area is necessary. The first step is to obtain the geochemical characteristics of shallow groundwater and soil systems. This is also important and necessary to understand the possible negative environmental impacts of shale gas production, especially the hydraulic fracturing processes on local shallow groundwater and soil systems before contamination occurs, not only for the domestic water supply, but also for establishing guidance for wide shale gas resources development in China.

In this study, water samples from 20 springs for the drinking water supply of the Jiaoshiba (JSB) region and five soil water samples were analyzed in an attempt to identify the geochemical characteristics of shallow groundwater systems and possible contamination. In order to be representative of the conditions of the production areas, these samples were collected both upstream and downstream of the shale gas production platform. Multiple geochemical and isotopic compositions together with their geospatial distribution were adopted to provide an approach to examine the shallow groundwater geochemical characteristics and potential contamination in the shale gas production areas. Shallow drinking water can be contaminated with deeper saline fluid leakage and stray gas migration associated with drilling and hydraulic fracturing due to poor well integrity, faults, and groundwater circulation [6,18]. This study is intended to report the comprehensive evaluation of the geochemical characteristics of the shallow groundwater due to shale gas production in the JSB region.

## 2. Study Area

The study area is located within the currently mostly active development area for shale gas production of the JSB area, southeast of the Sichuan basin (Figure 1). The area is characterized by a transitional zone between the Tibetan plateau and the middle-lower reaches of the Yangtze River plain, dominated by hilly areas. Due to the occurrence of the Qiyue fault, the region is divided into the internal and external area of the basin and the JSB block is in the internal area (Figure 1). It is a typically subtropical humid monsoon climate with a high annual average temperature of 16–19 °C. The annual average precipitation is 1000–1200 mm and 70% of the total precipitation is focused in May–September with rainstorms. Various rivers belonging to the Yangtze River system are developed in the JSB area and the main rivers are the Jialingjiang River, Wujiang River (WJR), and Dalinghe River.

Tectonically, the study area is located in the southeast of the upper Yangzi Plate and it is characterized as a typically passive continental margin [19,20]. Extensional and compressive faults of several kilometers are developed. Strata of the study area comprise the Precambrian clastic rock and dolomite, Ordovician (O) limestone, Silurian (S) shale, Permian (P) and Triassic (T) limestone [21] (Figure 1, A–B cross-section). Due to the self-sealing ability and the huge gap up to two to eight times between the vertical and lateral permeability of shale gas reservoirs, lateral diffusion is the basic pattern of shale gas migration in the area [22]. The Longmaxi (LMX) shale formation of the Silurian period is the target reservoir during drilling with an area of  $1.28 \times 10^4 \text{ km}^2$  and it lies approximately 2000–4000 m below the ground surface [23,24]. It is a series of clastic rock and carbonates mixing depositions with a thickness of 60–500 m and is demonstrated to be the most promising group of shale gas reservoirs in China. The upper formation mainly consists of mudstone with shallow water continental deposition facies; the middle part begins developing a muddy siltstone; the lower section is dominated by black shale developed in a deep-water continental sedimentary environment [25]. During the deposition of the LMX shale in a closed sea basin environment, abundant organic matter was incorporated into the sediment, forming a series of organic-rich black shale with the potential to produce hydrocarbons upon deep burial [26].

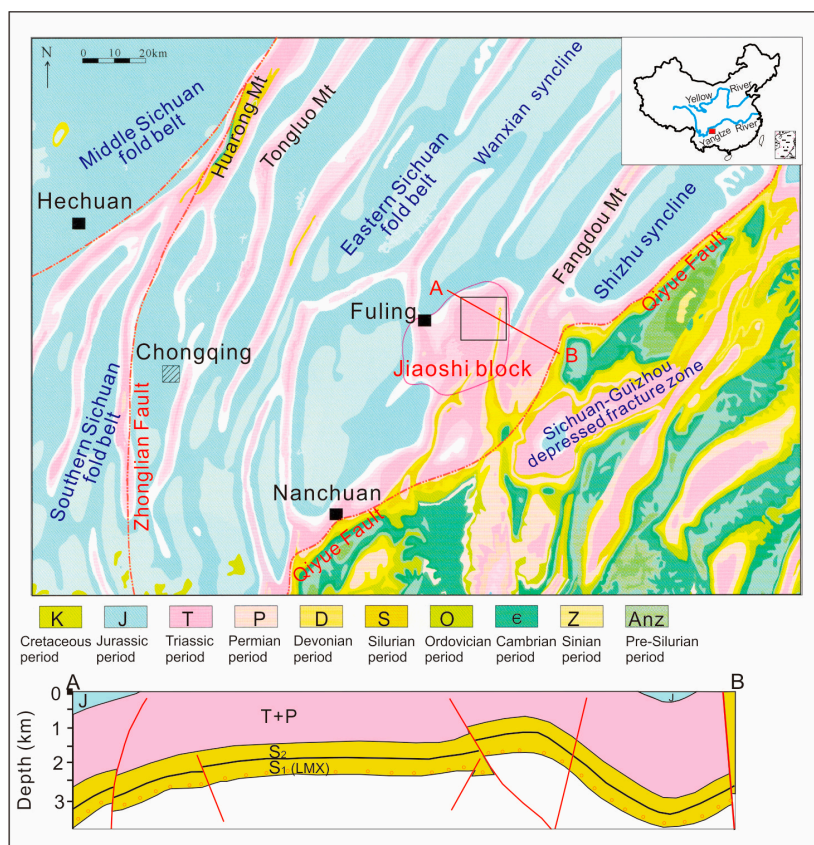
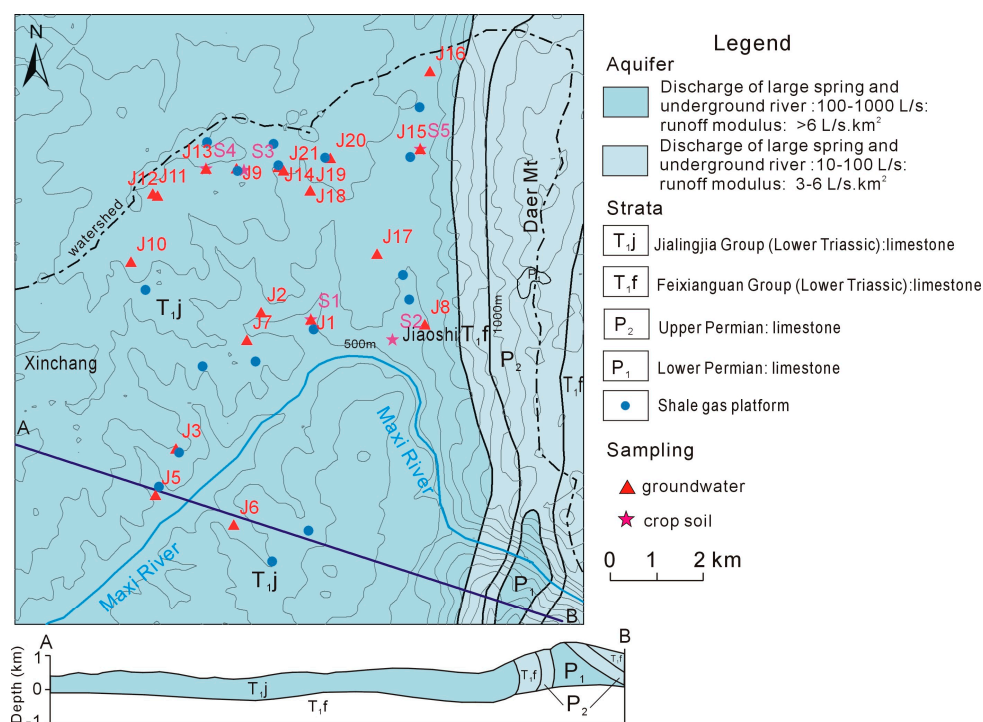


Figure 1. Regional geology and the sketch tectonics of the JSB block, modified from [12,22].

Importantly, the LMX shale is the first shale gas development in the study area and the JSB area is explored to be the first large-scale shale gas field with several hundreds of cubic gigameters ( $10^9$ ) of reserves, accounting for about 20% of the shale gas in China and more than five billion  $m^3$  of shale gas per year can be achieved [27]. Existing exploration wells and the presence of potential faults systems may provide possible conduits for the vertical migration of stray gas and hydraulic fracturing fluid. The exposed and shallow subsurface geological formations are a series of dominantly limestone formations, and the karst phenomenon is widely developed in the study area.

Carbon, pyrite, fossils of graptolite, benthic organisms, and siliceous radiolarian are abundant in the LMX shale, and lateral stratification is strongly developed, indicating great heterogeneity [28]. Long-term compaction processes and cementation lead to extremely low porosity and permeability. The porosity of the LMX black shale formation is 1.5%–2.5%, with an average value of 1.9%, and the permeability is  $1 \times 10^{-4}$ – $1.3 \times 10^{-3}$  mD, with an average value of  $7.6 \times 10^{-4}$  mD [12]. Various types of pores and fractures exist in the black shale, including micro-pores between particles, intraparticle pores, pores between clay minerals, structural fractures, and fractures formed during diagenesis.

The lithology of shallow groundwater aquifers is all limestone and dolomite, which are the Lower Triassic Jianglingjiang group ( $T_{1j}$ ) with a thickness of 277 m and the Feixianguan group ( $T_{1f}$ ) (426 m) and the Upper Permian group ( $P_2$ ) with a thickness of 226 m and the Lower Permian group ( $P_1$ ) (474 m) (based on the borehole of JY1). The shale gas exploitation field is mainly located in the middle and low mountainous area with a surface lithology of  $T_{1j}$ . Here the discharge of large springs and underground rivers ranges from 100 L/s to 1000 L/s and the runoff modulus is more than  $6 \text{ L/s}\cdot\text{km}^2$  (Figure 2). Although the lithology of the shallow aquifer is simple, the anisotropy is strong, causing the heterogeneous occurrence of groundwater and cave springs (outcropping of the karst groundwater) in the area. The shallow groundwater aquifer mainly distributes in the upper 150 m of the limestone [29].



**Figure 2.** Hydrogeological conditions and shallow groundwater and soil sampling location in the JSB area.

### 3. Samples and Methods

In order to investigate the hydrogeochemical characteristics of the shallow groundwater of karst aquifers, a total of 20 water samples were collected from karst springs in the JSB area in the southeast Sichuan basin in November 2014. In addition, methane concentrations of shallow groundwater were also analyzed. Water chemistry and isotopes have been analyzed within one month after sampling. The water sampling locations are shown in Figure 2. Physical and chemical parameters such as pH, temperature, conductivity and Eh were measured in situ using a multi-parameter device, HACH SENSION. All samples were filtered by a 0.45 μm membrane and kept in polypropylene (PP) bottles before analysis and samples for cation analysis were acidified with ultra-purified HNO<sub>3</sub> (1 mol/L) to adjust the pH to lower than 2. All of the water samples were stored in a refrigerator at 4 °C for proper preservation before analysis.

Water chemistry and trace element analysis were all performed in the Analytical Laboratory of the Beijing Research Institute of Uranium Geology (BRIUG), Beijing, China. Anions (F<sup>-</sup>, Cl<sup>-</sup>, SO<sub>4</sub><sup>2-</sup>, and NO<sub>3</sub><sup>-</sup>, detection limit is 0.1 mg/L) were measured with a DIONEX-500 Ion Chromatograph and HCO<sub>3</sub><sup>-</sup> by a 785 DMP titrator (accuracy is ±5 mg/L). Cations (K<sup>+</sup>, Na<sup>+</sup>, Ca<sup>2+</sup>, Mg<sup>2+</sup>) were quantitatively analyzed by Inductively Coupled Plasma Optical Emission Spectroscopy (ICP-OES, OPTIMA2X00/1500, BRIUG, Beijing, China) with a detection limit of 0.1 mg/L. Trace elements were determined by Inductively Coupled Plasma Mass Spectrometry (ICP-MS, BRIUG, Beijing, China). Stable isotopes (δ<sup>18</sup>O<sub>H2O</sub>, δ<sup>2</sup>H<sub>H2O</sub>) were analyzed by a laser absorption water isotope analyser Picarro L1102-i in the Water Isotope and Water-Rock Interaction Laboratory at the Institute of Geology and Geophysics, Chinese Academy of Sciences, Beijing, China. The precision of the δ<sup>18</sup>O<sub>H2O</sub> and δ<sup>2</sup>H<sub>H2O</sub> values were ±0.1‰ and ±0.5‰, respectively. δ<sup>13</sup>C and <sup>14</sup>C were analyzed by the radiocarbon laboratory of Beta Analytics with accuracies were ±0.1‰ and ±0.1 pmc, respectively. The <sup>3</sup>H contents were measured in the Analytical Laboratory of the (BRIUG), Beijing, China through electrolytic enrichment with a <sup>3</sup>H enrichment factor of ~20 and the liquid scintillation counting (Quantulus 1220) method. The precision of <sup>3</sup>H was ±0.4 TU.

Methane concentrations were analyzed for some water samples within one week after sampling. An approximate 2 mL aliquot of the headspace gas was removed with a gas-tight syringe and injected into a gas chromatograph for shallow groundwater methane content measurement in Shanghai SEP Analytical Service Co., Ltd, Shanghai, China, using the standard operating procedure of USEPA RSK 175-2004. The detection limit is 0.01 mg/L for methane.

The soil samples in crop fields were obtained using a shovel. Bulk samples of ~500 g were collected. Samples were immediately sealed in polyethylene bags. Gravimetric moisture content ( $\theta$ ) was determined by drying a minimum of 80 g of sediment at 110 °C for 12 h. For analysis of the nitrate concentrations, double-deionized water (40 mL) was added to the oven-dried sediment sample (40 g). Samples were agitated intermittently for 8 h. The supernatant solution was filtered through 0.45  $\mu\text{m}$  filters. Solutes were then analyzed by Ion Chromatography in the BRIUG, Beijing, China. The nitrate concentration of the soil solution is then calculated by dividing the measured concentration by gravimetric moisture content and by multiplying the mass ratio of solution over oven-dry sediment.

## 4. Results

### 4.1. Geochemical Characteristics of Shallow Groundwater System

The shallow groundwater samples were collected from springs of karst aquifers which are also used for the drinking water supply of local residents. Concentrations of major ions and stable isotopes, pH, and temperature are listed in Table 1. The charge balances of all the samples were  $\pm 3\%$  and satisfied the data quantity assurance. The water is neutral to slightly alkaline with an average pH of 7.5 (7.1–8.0). The amount of TDS varies from about 150 mg/L to 350 mg/L and the main constituents are  $\text{Ca}^{2+}$ ,  $\text{Mg}^{2+}$ , and  $\text{HCO}_3^-$ .  $\text{Ca}^{2+}$  and  $\text{Mg}^{2+}$  contents in the shallow groundwater range from 43 mg/L to 134 mg/L and 2.5 mg/L to 24.5 mg/L, respectively, taking 61–94 meq% and 7–36 meq% of the total cations (Table 1).  $\text{HCO}_3^-$  concentrations range from 142 mg/L to 358 mg/L and make dominant contributions to the anions. The  $\text{NO}_3^-$  content of shallow groundwater ranges from 2.5 mg/L to 78.3 mg/L and only two sample have an  $\text{NO}_3^-$  content exceeding the drinking water standard of China as 44 mg/L.  $\text{SO}_4^{2-}$  concentrations are much higher than  $\text{Cl}^-$  contents with contributions of 9–25 meq%. The main water types are  $\text{HCO}_3\text{-Ca}$  and  $\text{HCO}_3\text{-Ca-Mg}$  based on the Piper diagram analysis (Figure 3). While the value of 10–28 mg/L, the action level for hazard mitigation recommended by the US Office of the Interior [6], is used as the water quality standard, all groundwater methane contents are not detected—i.e., they are less than 0.01 mg/L. This suggests that all groundwater samples have not been affected by stray gases yet.

Results of trace elements show that concentrations of most of the heavy metals were very low and below the drinking water standards of China. The concentration of barium was 7–70  $\mu\text{g/L}$  and it is much higher than that of other elements.

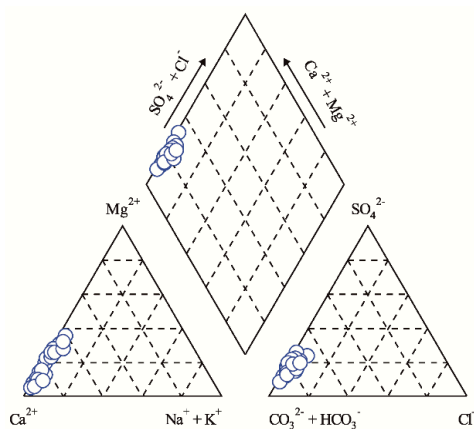


Figure 3. Piper diagram of shallow groundwater samples from karst aquifers.

**Table 1.** Geochemical and isotopic compositions of shallow groundwater in the JSB area.

Sample Number	pH	Ca <sup>2+</sup>	Mg <sup>2+</sup>	Na <sup>+</sup>	K <sup>+</sup>	HCO <sub>3</sub> <sup>−</sup>	F <sup>−</sup>	NO <sub>3</sub> <sup>−</sup>	Cl <sup>−</sup>	SO <sub>4</sub> <sup>2−</sup>	TDS	Water Type	δ <sup>18</sup> O <sub>H2O</sub>	δ <sup>2</sup> H <sub>H2O</sub>	δ <sup>13</sup> C <sub>DIC</sub>	<sup>14</sup> C	<sup>3</sup> H
		(mg/L)											(‰)		(pmc)	(TU)	
J1	8.0	95.0	8.5	4.8	3.6	260	0.1	27.1	10.9	38.5	291	HCO <sub>3</sub> -Ca	−6.7	−42.9	−11.7	95.4	6.5
J2	7.4	94.1	14.1	1.0	0.3	193	0.1	78.3	12.5	52.0	271	HCO <sub>3</sub> -Ca	−6.7	−42.2			
J3	7.7	81.4	7.9	0.8	0.9	204	0.2	9.6	2.0	55.8	251	HCO <sub>3</sub> -Ca	−6.9	−45.6			
J5	7.3	102	17.6	0.4	0.3	305	0.2	13.7	0.8	49.8	323	HCO <sub>3</sub> -Ca	−7.0	−44.0			
J6	7.7	69.8	24.5	3.1	2.5	239	0.3	9.2	10.2	53.7	283	HCO <sub>3</sub> -Ca·Mg	−6.9	−43.6	−15.1	98.4	8.6
J7	7.5	99.2	4.9	1.1	0.9	284	0.2	9.9	3.8	31.6	283	HCO <sub>3</sub> -Ca	−6.9	−43.8			
J8	7.7	61.9	11.5	1.0	1.3	182	0.2	5.4	2.1	38.0	207	HCO <sub>3</sub> -Ca	−7.6	−49.9	−14.6	98.6	7.4
J9	7.6	48.3	13.5	1.5	1.3	154	0.2	4.2	2.2	36.2	180	HCO <sub>3</sub> -Ca·Mg	−6.4	−44.0			
J10	7.7	85.4	6.3	0.9	0.8	248	0.1	6.2	1.5	26.6	245	HCO <sub>3</sub> -Ca	−6.9	−44.6			
J11	7.7	89.4	9.9	1.4	1.0	236	0.2	28.6	3.6	40.2	264	HCO <sub>3</sub> -Ca	−7.0	−43.4			
J12	7.9	86.2	5.8	2.1	1.8	221	0.1	31.1	4.0	40.0	251	HCO <sub>3</sub> -Ca	−7.2	−44.7			
J13	7.4	46.0	10.0	0.8	1.3	150	0.1	7.5	1.2	32.2	167	HCO <sub>3</sub> -Ca·Mg	−6.4	−43.8			
J14	7.2	134	4.3	1.3	1.0	358	0.4	31.5	3.5	27.1	350	HCO <sub>3</sub> -Ca	−7.4	−45.9			
J15	7.6	71.9	17.0	0.9	0.7	258	0.1	3.3	2.8	38.9	261	HCO <sub>3</sub> -Ca·Mg	−6.9	−42.7			
J16	7.1	43.5	9.2	0.5	0.7	142	0.1	3.1	0.6	26.7	152	HCO <sub>3</sub> -Ca·Mg	−5.8	−40.2	−12.8	97.4	7.3
J17	7.7	68.8	2.5	1.1	1.5	198	0.2	2.5	2.6	25.1	201	HCO <sub>3</sub> -Ca	−6.4	−40.3			
J18	7.6	70.5	15.4	2.2	1.6	238	0.1	25.6	4.7	28.5	242	HCO <sub>3</sub> -Ca·Mg	−7.2	−44.6			
J19	7.2	85.4	21.7	7.6	3.3	286	0.2	23.7	12.4	45.6	319	HCO <sub>3</sub> -Ca·Mg	−6.9	−43.5			
J20	7.2	80.9	24.5	3.6	2.8	273	0.2	27.4	5.0	52.1	305	HCO <sub>3</sub> -Ca·Mg	−6.7	−40.8			
J21	7.7	110	6.9	5.1	4.1	234	0.1	71.4	11.6	48.4	303	HCO <sub>3</sub> -Ca	−7.2	−43.2			

#### 4.2. Isotope Characteristics ( $\delta^{18}\text{O}_{\text{H}_2\text{O}}$ , $\delta^2\text{H}_{\text{H}_2\text{O}}$ , $\delta^{13}\text{C}$ , $^{14}\text{C}$ ) of Shallow Groundwater System

The water isotopes of  $\delta^{18}\text{O}_{\text{H}_2\text{O}}$  and  $\delta^2\text{H}_{\text{H}_2\text{O}}$  are analyzed to be  $-5.8\text{‰}$ – $-7.6\text{‰}$  and  $-40.2\text{‰}$ – $-49.9\text{‰}$ , respectively (Table 1). With respect to their isotopic compositions, all the shallow groundwater samples lie around the Local Meteoric Water Line (LWML) which is obtained from the isotopic data of Chengdu station of the International Atomic Energy Agency database, indicating that it is recharged by the local precipitation in the region (Figure 4). The distribution of the stable isotopes of shallow groundwater also indicates quick circulation.

Carbon isotope measurement can be used to trace the sources and geochemical processes of dissolved inorganic carbon (DIC) in the groundwater. Results show that the  $\delta^{13}\text{C}_{\text{DIC}}$  ranges from  $-11.7\text{‰}$  to  $-15.1\text{‰}$ , with an average value of  $-13.6\text{‰}$  (Table 1). Groundwaters have relatively high  $^3\text{H}$  values ranging from 6.5 TU to 8.6 TU. The  $^{14}\text{C}$  content of shallow groundwater varies from 95.4 pmc (percentage of modern carbon) to 98.6 pmc with an average value of 97.5 pmc. The detected  $^3\text{H}$  and high  $^{14}\text{C}$  content indicate a young age of the groundwater and quick circulation.

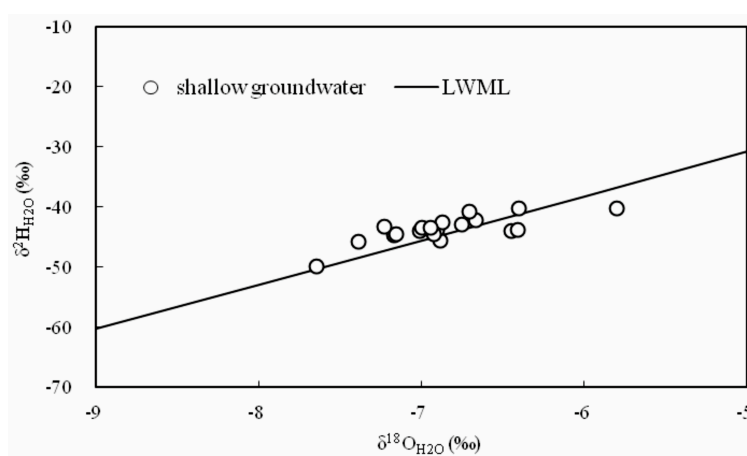


**Figure 4.** Stable isotopes of shallow groundwater and its relationship with the local water meteoric line.

#### 4.3. Geochemical Characteristics of Soil System

Five soil samples are collected and analyzed. The soil compositions are limited to the weathering extent, the mineral compositions of which are mainly quartz, K-feldspar, calcite, dolomite, and clay minerals (Table 2). Taking soil sample S5, collected in the north of the JSB area, as an example, it is greatly influenced by weathering and all the carbonate minerals in the parent rock are consumed, resulting in the contents of the clay minerals increasing. The nitrate concentrations in the soil water vary from 3 mg/L to 416 mg/L with an average value of 106 mg/L, most of which are higher than the drinking water standard GB5749-2006 of 44 mg/L and also the III level standard of groundwater quality of 88 mg/L of China. Generally, the background nitrate concentration is less than 12 mg/L [30] and much higher nitrate concentrations are mainly caused by local agricultural activities.

**Table 2.** Mineral compositions of soil samples in the JSB area.

Sample Number	Quartz	K-Feldspar	Calcite	Dolomite	Clay Minerals	$\text{NO}_3^-$ of Soil Water (mg/L)
	(wt %)					
S1	50.6	/	15.4	/	34.0	3
S2	61.4	/	10.7	3.3	24.6	416
S3	65.3	3.5	5.3	/	25.9	63
S4	54.7	3.8	7.7	2.2	31.6	5
S5	64.5	2.1	/	/	33.4	43

## 5. Discussion

### 5.1. Geochemical Characteristics of Shallow Groundwater System

Baseline study is important and necessary to detect whether the groundwater is contaminated and to what extent. Generally, monitoring should be carried out five to six years before shale gas production. However, the pity is that shallow groundwater system baseline investigations are being performed after shale gas production in the JSB area. Therefore, those groundwater samples are collected around shale gas production areas to be representative as geochemical characteristics of shallow groundwater systems.

Boxplots are used to assess the statistical characteristics of shallow groundwater based on the unbiased estimation principle. The median value, maximum value, minimum value, 75th percentile, and 25th percentile of shallow groundwater samples are clearly shown in Figure 5a,b for major ions and trace elements. Most of the major ions satisfy the drinking water standard GB5749-2006 applied in China, except the nitrate concentrations of some of the samples (e.g., J2, J21) are higher than 44 mg/L. This is also observed in the soil water samples and it is inferred to be caused by agricultural pollution and it is not related to shale gas production. Concentrations of typical toxicity indexes including Mn, Cr, Cu, Zn, Ba, and Pb are all below the drinking water standard (Figure 5b).

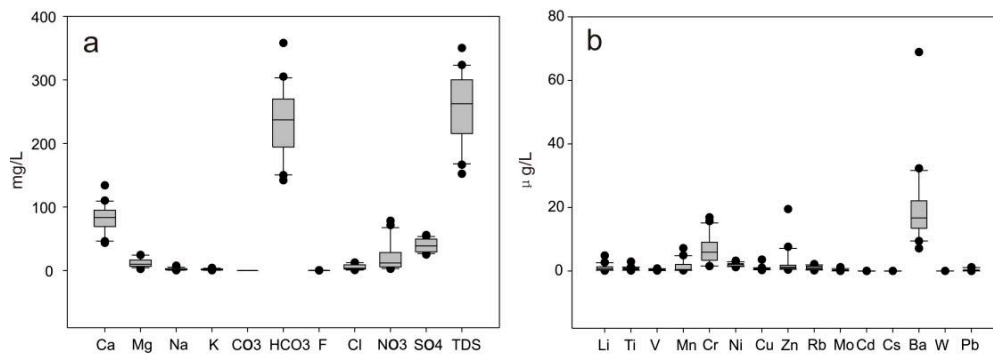
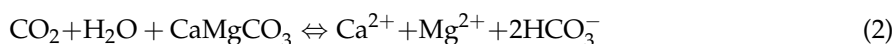


**Figure 5.** (a) Geochemical characteristics of major ions and (b) trace elements of shallow groundwater based on boxplot method.

### 5.2. Geochemical Reactions

The low TDS and  $\text{HCO}_3\text{-Ca}$  and  $\text{HCO}_3\text{-Ca}\cdot\text{Mg}$  water types of the shallow groundwater suggest a typical geochemical characteristics and mode of the water-rock interaction of karst aquifers. The low-TDS waters reflect an early stage of groundwater recharge without much mineralization induced by the water-rock interaction, while  $\text{HCO}_3\text{-Ca}$  and  $\text{HCO}_3\text{-Ca}\cdot\text{Mg}$  water types suggest the dissolution of carbonate minerals in the karst aquifers as presented by Equations (1) and (2). The saturation index (SI) calculation is conducted by geochemical software PHREEQC 3.0 and *lnl.dat* [31]. Results show that most of the samples are over-saturated with respect to calcite and dolomite whose SI range from 0.07 to 0.83 and 0.05 to 1.98, respectively.

In the majority of the shallow groundwater samples, the  $\text{Na}^+$  content is lower than 11.5 mg/L. The DIC in the shallow groundwater can be generated by the weathering of silicate minerals, the dissolution of marine carbonates, or bacterial sulfate reduction [3]. Because the shallow aquifers are composed of Triassic carbonates, the dissolution of marine carbonate may be the dominant source s of DIC as illustrated by Equations (1) and (2). The  $\delta^{13}\text{C}_{\text{DIC}}$  value could reflect the isotopic fractionation between DIC species and if the dissolution of carbonate minerals was occurring, one would expect a DIC with a  $\delta^{13}\text{C}_{\text{DIC}}$  value of  $-15.1\text{‰}$ , assuming an open system with equal proportions of carbonate dissolution ( $\delta^{13}\text{C}_{\text{DIC}}$ ,  $0\text{‰}$ ) and soil  $\text{CO}_2$  ( $\delta^{13}\text{C}_{\text{DIC}}$ ,  $-23\text{‰}$ ) at  $25\text{ °C}$ , with all the DIC-bearing species in an isotopic equilibrium. Therefore, carbonate dissolution is the major geochemical process that controls the generation of  $\text{HCO}_3\text{-Ca}$  and  $\text{HCO}_3\text{-Ca}\cdot\text{Mg}$  water for the shallow groundwater system.



### 5.3. Circulation and Renewability of the Shallow Groundwater System

The aquifer of the shallow groundwater system in the JSB area is composed of limestone of the Triassic Jialingjiang group and the Badong group, and various karst systems are developed, including various cave systems. The water table in the karst area is generally less than 50 m and underground rivers are widely developed in depressions and valleys. Hydraulic connections between the surface water and groundwater are close and transition occurs frequently. One thing that needs to be mentioned is that the water quantity varies greatly between dry and wet periods, differences of which can be up to 10 to 50 times.

Vertically, the shallow karst aquifers can be divided into three zones, the vertical circulation zone, the horizontal circulation zone, and the deep circulation zone, respectively (Figure 6). In the vertical circulation zone, groundwater circulation is quick and has strong connections with the surface water. All the shallow groundwater samples belong to the vertical circulation zone, indicating a quick circulation path.

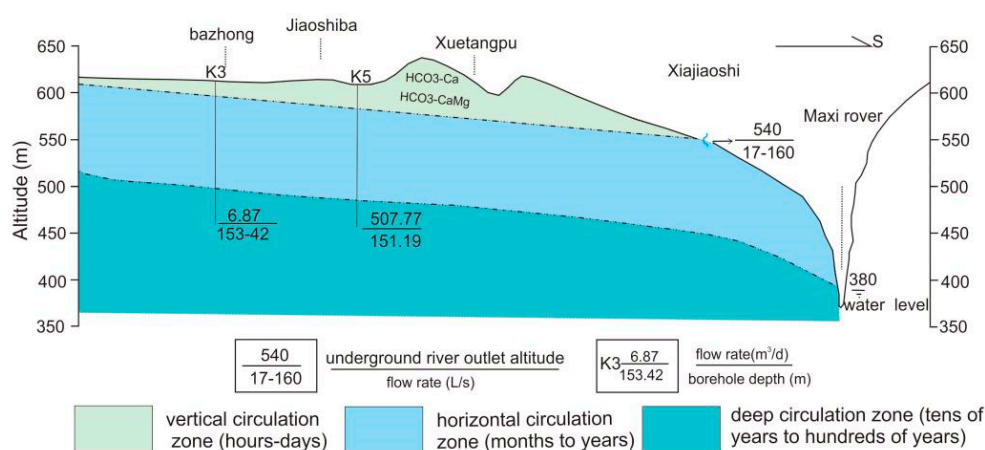


Figure 6. Hydrogeological cross-section and circulation depth of karst aquifers in the JSB areas.

The high <sup>3</sup>H (6.5–8.6 TU) and <sup>14</sup>C content of shallow groundwater (95.4–98.6 pmc) indicate that it is modern water with a quick circulation rate and strong renewability. The δ<sup>13</sup>C<sub>DIC</sub> of karst water shows typical characteristics of dissolution equilibrium between CO<sub>2</sub> and carbonates in an open system as presented by Equation (1), where δ<sup>13</sup>C values of CO<sub>2</sub>, CaCO<sub>3</sub>, and HCO<sub>3</sub> are −23‰, 0‰, and −15.1‰, respectively, for the equilibrium state of the open system. This is also verified by the water isotopes that are located around the LWML which indicate that precipitation recharges the shallow karst groundwater system as soon as it happens and evaporation can be ignored (Figure 4). The low TDS (<350 mg/L) and water types of HCO<sub>3</sub>-Ca and HCO<sub>3</sub>-Ca·Mg provide additional evidence that the circulation of shallow groundwater is quick and strong hydraulic connections among various karst areas can be identified. If water pollution from deep shale gas production happens, two important aspects should be mentioned: on one hand, the self-recovering ability of the shallow groundwater system is strong; however, on the other hand, the whole groundwater system will be polluted due to the excellent hydraulic conditions.

## 6. Conclusions

The geochemical characteristics of the shallow groundwater system and soil system have been investigated and established by statistical analysis of major and trace elements in one of the most important shale gas production areas in China. The shallow groundwater is karst water with low TDS, less than 350 mg/L. The main water types are  $\text{HCO}_3\text{-Ca}$  and  $\text{HCO}_3\text{-Ca}\cdot\text{Mg}$  due to carbonate dissolution equilibrium in the karst reservoirs. The concentrations of most of the major ions and typical toxicity indexes (Mn, Cr, Cu, Zn, Ba, and Pb) satisfy the drinking water standard GB5749-2006. High concentrations of  $\text{NO}_3^-$  in some samples, especially in soil water samples, are attributed to agricultural pollution and are not related to shale gas production.

The shallow groundwater system is hydrogeologically in the vertical circulation zone of the karst aquifer and is recharged by local precipitation. Modifications of chemical compositions are attributed to carbonate dissolution along the flow paths in the shallow aquifers. Low TDS and high contents of  $^3\text{H}$  and  $^{14}\text{C}$  indicate a quick and efficient circulation and strong renewability of the shallow groundwater system. Once pollution from shale gas production occurs, the shallow groundwater system will be contaminated as soon as possible and, furthermore, it will be recovered soon due to quick circulation by precipitation.

**Acknowledgments:** This work is supported by the “Strategic Priority Research Program (B)” of the Chinese Academy of Sciences (Grant XDB10030603) and the National Natural Science Foundation of China (Grant 41402236). We are indebted to two anonymous reviewers and Editor for their thoughtful comments that improved the quality of the paper.

**Author Contributions:** Tianming Huang and Yingchun Wang visited the field site of Jiaoshiba and sampled the shallow groundwater samples and soil samples. Yiman Li performed the water chemistry analysis; Chao Jin carried out the soil water preparation and nitrate analysis; Yiman Li wrote the paper; and Tianming Huang and Zhonghe Pang provided suggestions for modification of the manuscript.

**Conflicts of Interest:** The authors declare no conflict of interest.

## References

1. Joseph, H.; Frantz, J.; Jochen, J.V. *Shale Gas White Paper*; Schlumberger Marketing Communications: New York, NY, USA, 2005; pp. 1–9.
2. Zolfaghari, A.; Noel, M.; Dehghanpour, H.; Bearinger, D. Laboratory and Field Analysis of Flowback Water from Gas Shales. *J. Unconv. Oil Gas Resour.* **2016**, *14*, 113–127. [[CrossRef](#)]
3. Warner, N.R.; Kresse, T.M.; Hays, P.D.; Down, A.; Karr, J.D.; Jackson, R.B.; Vengosh, A. Geochemical and isotopic variations in shallow groundwater in areas of the Fayetteville Shale development, north-central Arkansas. *Appl. Geochem.* **2013**, *35*, 207–220. [[CrossRef](#)]
4. Gregory, K.B.; Vidic, R.D.; Dzombak, D.A. Water management challenges associated with the production of shale gas by hydraulic fracturing. *Elements* **2011**, *7*, 181–186. [[CrossRef](#)]
5. Howarth, R.; Ingraffea, A.; Engelder, T. Natural gas, should fracking stop? *Nature* **2011**, *477*, 271–275. [[CrossRef](#)] [[PubMed](#)]
6. Osborn, S.G.; Vengosh, A.; Warner, N.R.; Jackson, R.B. Methane contamination of drinking water accompanying gas-well drilling and hydraulic fracturing. *Proc. Natl. Acad. Sci. USA* **2011**, *108*, 8172–8176. [[CrossRef](#)] [[PubMed](#)]
7. Hayes, T. *Sampling and Analysis of Water Streams Associated with the Development of Marcellus Shale Gas*; Gas Technology Institute: Des Plaines, IL, USA, 2009; pp. 1–210.
8. Kharak, Y.K.; Thordsen, J.J.; Conaway, C.H.; Thomas, R.B. The energy-water Nexus, Potential groundwater-quality degradation associated with production of shale gas. *Procedia Earth Planet. Sci.* **2013**, *7*, 417–422. [[CrossRef](#)]
9. Rowan, E.L.; Engle, M.A.; Kirby, C.S.; Kraemer, T.F. *Radium Content of Oil- and Gas-field Produced Waters in the Northern Appalachian Basin (USA), Summary and Discussion of Data*; Report 2011; U.S. Geological Survey Scientific Investment: Reston, VA, USA, 2011; pp. 2011–5135.
10. Haluszczak, L.O.; Rose, A.W.; Kump, L.R. Geochemical evaluation of flowback brine from Marcellus gas wells in Pennsylvania, USA. *Appl. Geochem.* **2013**, *28*, 55–61. [[CrossRef](#)]

11. Pritz, M.E.; Kirby, C.S. Geochemical investigation of Marcellus Shale natural gas hydrofracturing waters. *Geol. Soc. Am. Abstr. Prog.* **2010**, *42*, 121.
12. Guo, T.L.; Zhang, H.R. Formation and enrichment mode of Jiaoshi shale gas field, Sichuan Basin. *Pet. Explor. Dev.* **2014**, *41*, 28–36. (In Chinese) [[CrossRef](#)]
13. Zou, C.N.; Dong, D.Z.; Wang, Y.M.; Li, X.J.; Huang, J.L.; Wang, S.F.; Guan, Q.Z.; Zhang, C.C.; Wang, H.Y.; Liu, H.L.; et al. Shale gas in China, characteristics, challenges and prospects (II). *Pet. Explor. Dev.* **2016**, *43*, 166–178. (In Chinese) [[CrossRef](#)]
14. Dong, D.Z.; Zou, C.N.; Li, J.Z.; Wang, S.J.; Li, X.J.; Wang, Y.M.; Li, D.H.; Huang, J.L. Resource potential, exploration and development of prospect of shale gas in the whole world. *Geol. Bull. China* **2011**, *30*, 324–336. (In Chinese)
15. Dong, D.Z.; Gao, S.K.; Huang, J.L.; Guan, Q.Z.; Wang, S.F.; Wang, Y.M. A discussion on the shale gas exploration & development prospect in the Sichuan Basin. *Nat. Gas Technol.* **2014**, *34*, 1–15. (In Chinese)
16. Guo, X.S. *Shale Gas Enrichment Mechanism and Exploration Technology in Jiaoshi Block of Fuling Gas Field*; Science Press: Beijing, China, 2009. (In Chinese)
17. Wang, Z.G. Breakthrough of Fuling shale gas exploration and development and its inspiration. *Oil Gas Geol.* **2015**, *36*, 1–6. (In Chinese)
18. Warner, N.R.; Jackson, R.B.; Darrah, T.H.; Osborn, S.G.; Down, A.; Zhao, K.; White, A.; Vengosh, A. Geochemical evidence for possible natural migration of Marcellus Formation brine to shallow aquifers in Pennsylvania. *Proc. Natl. Acad. Sci. USA* **2012**, *109*, 11961–11966. [[CrossRef](#)] [[PubMed](#)]
19. Wang, H.Z. *Geology Development in South China*; Wuhan Geology Institute Press: Wuhan, China, 1985. (In Chinese)
20. Su, W.B. *Ordovician Sequence Stratigraphy and Sea Level Variations Study of the Upper Yangtze Platform*; Science Press: Beijing, China, 2009. (In Chinese)
21. Ma, Y.S.; Chen, H.D.; Wang, G.L. *Sequence Stratigraphy and Paleogeography in South China*; Science Press: Beijing, China, 2009. (In Chinese)
22. Hu, D.F.; Zhang, H.R.; Ni, K.; Yu, G.C. Main controlling factors for gas preservation conditions of marine shales in southeastern margins of the Sichuan Basin. *Nat. Gas Ind.* **2014**, *34*, 17–23. (In Chinese)
23. Liu, S.G.; Zeng, X.L.; Huang, W.M.; Ma, W.X. Basic characteristics of shale and continuous-discontinuous transition gas reservoirs in Sichuan Basin, China. *J. Chengdu Univ. Technol. (Sci. Technol. Ed.)* **2009**, *36*, 578–592. (In Chinese)
24. Wang, S.Q.; Chen, G.S.; Dong, D.Z.; Yang, G.; Lu, Z.G.; Xu, Y.H.; Huang, Y.B. Accumulation conditions and exploitation prospect of shale gas in the lower Paleozoic Sichuan basin. *Nat. Gas Ind.* **2009**, *29*, 51–58. (In Chinese)
25. Zou, C.N.; Dong, D.Z.; Yang, H.; Wang, Y.M.; Huang, J.L.; Wang, S.F.; Fu, C.X. Conditions of shale gas accumulation and exploration practices in China. *Nat. Gas Ind.* **2011**, *12*, 26–39. (In Chinese)
26. Zhai, Y.J. Shale gas Accumulation Conditions and Favorable Areas Forecast of Lower Silurian in East Chongqing. Master's Thesis, China University of Geosciences, Beijing, China, 2014. (In Chinese)
27. Yan, B. The First Large Scale Shale Gas Field is Born and Begin to Commercially Develop. July 2014. Available online: <http://china.haiwainet.cn> (accessed on 17 July 2014). (In Chinese)
28. Wang, Y.M.; Dong, D.Z.; Li, J.Z.; Wang, S.J.; Li, X.J.; Wang, L.; Cheng, K.M.; Huang, J.L. Reservoir characteristics of Longmaxi formation of the lower Silurian, Southern Sichuan. *Acta Petrol. Sin.* **2012**, *33*, 551–561. (In Chinese)
29. Lv, Y.X.; Hu, W.; Zhou, J. Analysis on karst development law and its influencing factors in Jiaoshi area of Chongqing city. *Chin. J. Geol. Hazard Control* **2012**, *23*, 59–63. (In Chinese)
30. Edmunds, W.M.; Shand, P. Groundwater baseline quality. In *Natural Groundwater Quality*; Edmunds, W.M., Shand, P., Eds.; Wiley: New York, NY, USA, 2008; pp. 1–21.
31. Parkhurst, D.L.; Appelo, C.A.J. *Description of Input and Examples for PHREEQC Version 3—A Computer Program for Speciation, Batch-Reaction, One-Dimensional Transport, and Inverse Geochemical Calculations*; U.S. Geological Survey Techniques and Methods: Denver, CO, USA, 2013; Book 6, Chapter A43, p. 497.

